Microstructural Investigation of Zirconium Alloys Subjected to Electron, Light and Heavy Ions Irradiations

R. Tewari, B. Vishwanadh, P. Mukharjee+, D. Srivastava, P. Barat+ and G. K. Dey
Materials Science Division, Bhabha Atomic Research Centre, Trombay, Mumbai 400 085, India
+Variable Energy Cyclotron Centre, 1/AF Bidhannagar, Kolkata 700 064, India
Email: rtewaribarc@yahoo.co.in

Abstract In the present study, microstructures have been examined in samples of zirconium based alloys irradiated with electron, protons and oxygen ions. In case of oxygen ion irradiation zircaloy-2 have been irradiated by O^{5+} ions with 116 MeV energy with different fluences varying from 10^{13} ion/cm^2 to 10^{15} ion/cm^2 and the effect of the irradiation has been studied in terms of the defect introduced into the materials. In the Zr-20Nb alloy, the formation of the ω phase under electron irradiation has been examined in a Zr-20 %Nb alloy. Samples were exposed to IMeV electrons and SAD patterns were recorded after different durations of irradiation at various temperatures and the formation of diffuse omega maxima has been noticed. The formation of the crystalline ω phase on prolonged irradiation and thermal treatment and its subsequent distribution has also been examined. In case of proton irradiation, the Zr-1Nb alloy has been irradiated with 8 MeV H^+ ions with fluence of 10^{10} ion/cm^2. As this energy of proton was higher than the coulombic barrier of the Zr ions, bombardment of protons led into the transmutation of Zr atoms into Nb atoms. Microstructural examination of such samples revealed interesting morphology of the β phase (bcc) in the α matrix.

1. Introduction

The irradiating particles impart energy to the target materials by the process of ionization, electronic excitation, displacement of atoms from the lattice, etc. Each of these processes of energy transfer is a function of type of ions, energy of the ions and the nature of target materials [1-4]. The energy transferred to materials is restored in terms of generation of interstitial and vacancy defects, which upon increasing concentration interact in many ways forming deferent kind of defects into the materials [1]. In place of ions, bombardment of electrons on materials causes the electronic excitement of the material which, in turn, induces phase transformation in the material. Some of these phase transformations are detrimental from the fracture strength point of view. The formation of the ω phase transformation is one such phase transformation. As pointed out by de Fontaine, the structure of the ω phase can be visualized by viewing a bcc unit cell along a <111> direction and giving a periodic displacement of the two successive atoms by 1/3 + u and 1/3 –u along <111> direction without moving the third atom. The variable 'u' can attain any value between 0 and 1/6. The former value of u represents the ideal ω structure and later the parent bcc structure. The values of u between 0 and 1/6 represent an intermediate structure which can be visualized as ω like fluctuations present in the parent β phase. The ω phase can be induced during irradiation in the β phase present in the Zr-2.5 Nb alloy. In the present study, therefore, an alloy of Zr-20Nb composition, which is the composition of the β phase generally encountered in the Zr-2.5 Nb alloy, was selected.

Effect of damage produced by heavy ions in nuclear reactor structural materials has been extensively studied [5-9]. One of the main incentives of using heavy ion irradiation technique is the substantial reduction in the experimental time. If the majority of the defects produced by heavy ions are similar to the defects produced by neutrons, these simulation studies provide important insight into the nature of the displacement damage produced [10]. These experiments can also be used to study the single isolated test variables [11]. For example, defects induced by neutrons irradiation, such as voids, swelling, dislocations loops, etc., can be selectively induced by selecting the appropriate ions for irradiation [12].

Studies on the void formation in zirconium based alloys upon irradiation with ions of noble gases, He, Kr [7,13-15] are plenty in number. In contrast, defects produced by reactive ions like, O, N, which form stable phase with the zirconium alloys, are very few [16,17]. In the present study attempts have been made to examine the microstructures of the irradiated materials by O^{+5} ions, by protons and electrons. Present paper deals with the microstructural changes observed upon irradiation with the O^{+5} ions with varying fluence and attempts have been made to study the kind of defects it generates in these alloys; as the path transverse by these ions it shows variety of the defects produced. Present paper also deals with the microstructural changes observed upon irradiation with H^+ ions with varying fluence and attempts have been made to study the kind of defects it generates in Zr based alloys. In addition it has also been shown that ω related phase transformation can be accelerated using high energy electron irradiation.

2. Experimental Procedure

Annealed thin sheets of dimensions 3cm x 5cm of Zircaloy-2 were irradiated with O^{5+} ion beam (with average energy 116 MeV energy) in variable energy cyclotron centre (VECC), Kolkata. These samples were exposed to a fluence of 1×10^{13}, 5×10^{13} and 1×10^{15} ions/cm^2.Subsequent to irradiation experiments, discs of 3 mm diameters were punched out from those regions of samples which were exposed to radiations. These discs were jet thinned by using electrolyte containing 20% perchloric acid and 80% methanol. The applied voltage was kept at 20 D C volts and the temperature of the bath was maintained at 243 K through out the thinning process. In addition, electron transparent wafers were cut out using focus ion beam from the regions exposed to ions. The depth of the ion implantation was estimated using SRIM program.
In another set of experiment electron transparent 3 mm discs of the alloy were directly subjected to proton irradiation in FOTIA BARC, Mumbai after examining them under transmission electron microscopy. For electron irradiation experiments, samples of the Zr-20Nb alloy were subjected to electron irradiation by using 1 MeV electrons. The electron irradiation was carried out in an AEI HVEM. Electron irradiation. The progress of the decomposition of the metastable β-phase under electron irradiation was monitored by examining the development of diffuse ω intensity distribution and/or shift of diffraction spots from the commensurate crystalline ω structure in a particular zone in the electron diffraction pattern of the β phase. A three dimensional bcc lattice of the β-Zr was created with 128x128x128 lattice points (~10^6 lattice points).The embryos of ω were generated by locally changing the coordinates of the atoms in the bcc unit cell The simulations were carried out with different ω number densities, aspect ratios to generate the corresponding SADs. In each simulation two possible ways of generating the ω structural subunits like ω_3, ω_5, ω_7 inside each ω embryo were tried. In one case, subunits were generated to have a particular sequence of ω_3, ω_5, ω_7, refereed here after as "Ordered", while in other case, the sequence of ω_3,ω_5,ω_7 is random,

3. Results

3. 1 Formation of Irradiation Induced Defects

Fig. 1 shows representative microstructures of the well annealed samples of the zircaloy and Zr-Nb alloys. Presence of high density of defects could be noticed from samples irradiated by oxygen ions to a fluence of 1×10^{13} ions/cm^2(Fig.2(a)). Similar microstructures with minor variations were observed in all the samples with increasing irradiation fluence. Presence of very fine regions (~10nm) with uniform distribution were also noticed in all the samples (Fig.2(b&c)). Tilting experiments revealed that defects have tendency to align and under certain tilt angle band like structure could be observed in most of the regions (Fig.2 (d)).

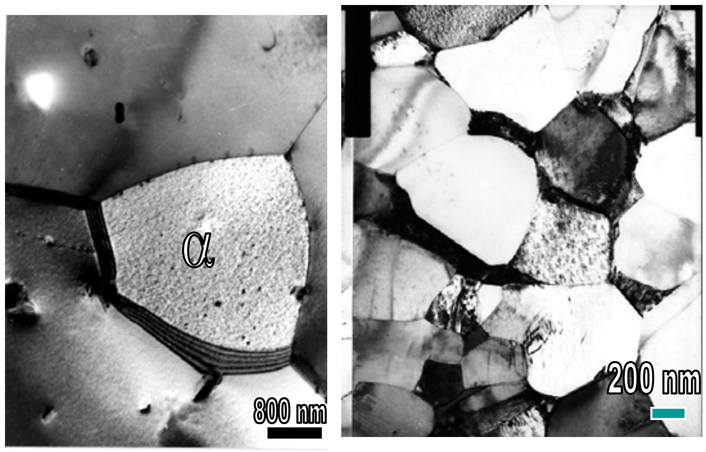

Fig.1 Typical annealed microstructure of the Zircaloy-2 specimen. Equiaxis grains and presence of the precipitate phase could be noticed from the micrograph.

Systematic tilting revealed presence of streaks in diffraction patterns which were oriented normal to these bands like structures (inset in Fig.2(d)). Since these diffuse streaks were not related to any of reflection from the matrix phase, there is a strong possibility that these streaks could be due to the align defects which could be solute atoms, It is worth mentioning that such bands were not noticed in any of the unirradiated samples. In order to confirm that such defects did not induce during sample preparation, samples of the unirradiated materials were also prepared under nearly identical conditions and examined under TEM. Unirradiated microstructure of Zircaloy showed did not show presence of such defects in the α (hcp) phase (Fig.1). A cross sectional examination of the region clearly showed regions of ions tracks in samples exposed to irradiation of fluence of 1 x 10^{15} ions/cm^2. Fig.3 showed the presence of such tracks. In the Zr-1Nb alloy upon irradiation with O^{+5} irradiation, in addition to the high dislocation density several places, formation of low angle grain boundaries and alignment of dislocations across the grain was observed. β-precipitates in the microstructure of the alloy, which invariably exhibit spherical morphology under annealed condition, showed elongated morphology indicating dissolution and reprecipitation of the phase under the influence of irradiation (Fig.4).
In case of proton irradiation experiments, considerable amount of defects were produced. The defects appear to have wider distribution than those observed in the case of O^{+5} ions exposed samples and in addition to these defects presence of very fine precipitates uniformly distributed in some of the grains (Fig. 5)

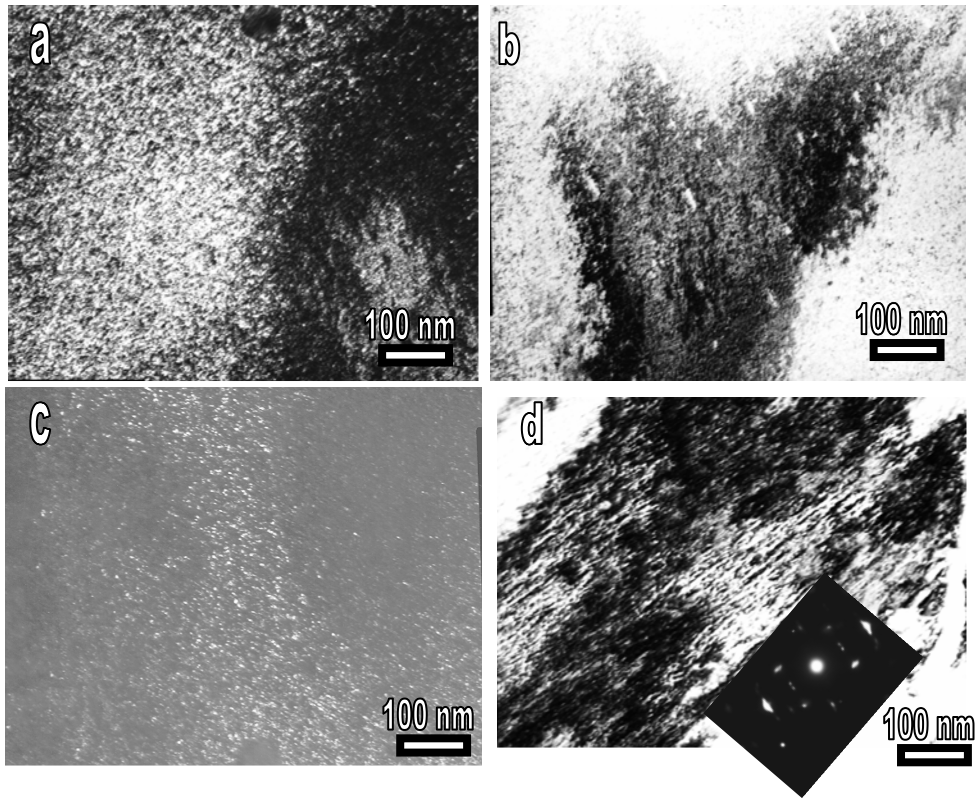

Fig.2 Typical microstructure of the Zircaloy-2 specimen after irradiated with O^{+5} ions for a fluence $1x10^{13}$ ions/cm^2. (a) Microstructure showing the presence of defects, (b) showing presence of precipitates in the microstructure, (c) dark field micrograph showing fine distribution of the precipitate in the α matrix and (d) The alignment of the defects could be noticed. SAD in inset shows the diffuse intensity around the $(10\bar{1}0)_\alpha$ reflection in direction perpendicular to bands. Image was taken when sample was away from the $[1\bar{2}10]$ zone.

.

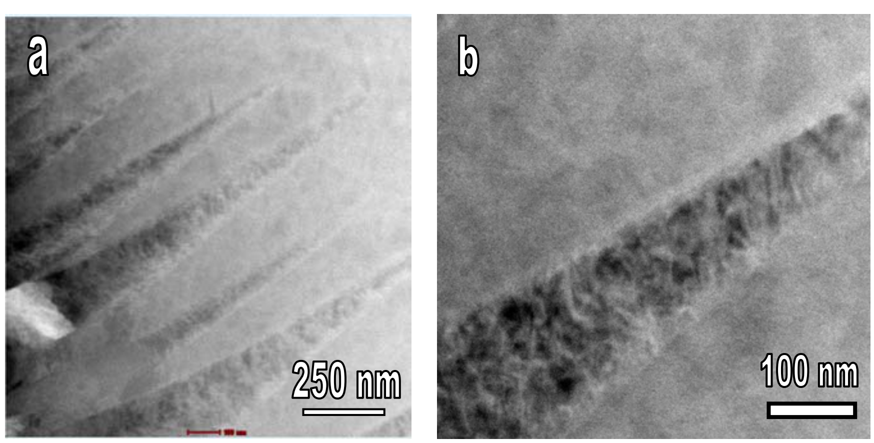

Fig.3 HADDF Micrographs showing tracks of O^{+5} ion in the samples of Zircaloy-2. (a) The contrast variation is due to the defect generated in high angle annular dark field images. (b) A magnified view of the one of such track.

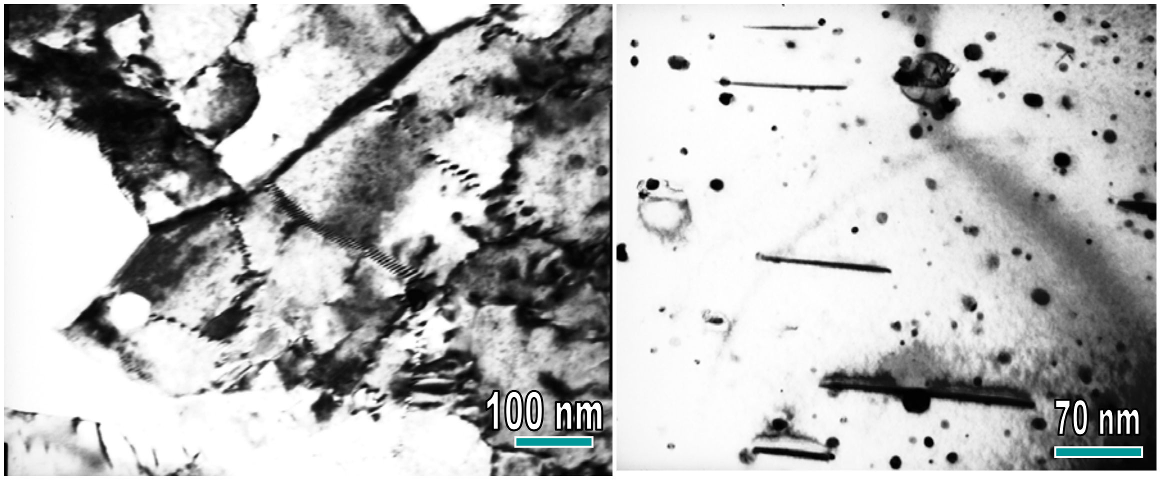

Fig. 4 Typical micrographs showing the presence of defects in Zr-1Nb alloy subsequent to O^{+5} irradiation

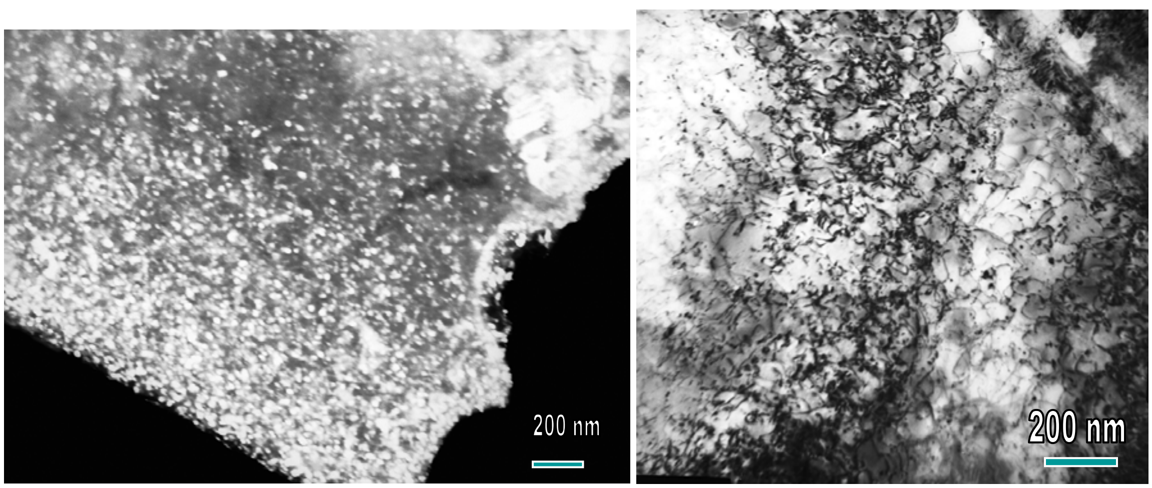

Fig. 5 Typical micrographs showing the presence of defects in Zircaloy-2 subsequent to H^{+} irradiation

4. Discussion

Studies have shown that in case of extremely low doses (< 10^{10} ion/cm^2), details of the defects generated can not be identified readily, as majority of the defects generated are too small in size and are, in general, randomly oriented [20]. On the other hand, extremely high doses (>10^{21} ions/cm^2) generate very high defect density that modifies the basic structure as these defects start interacting and producing secondary effects. Hence intermediate doses (10^{13-15} ions/cm^2) are most suited to study the changes induced in the microstructures by irradiation. Effects of the irradiation in this intermediate dose range have been observed in terms of array of dislocations [2,21,22], bands [11,17, 23], dislocation loops [2,24] etc. Most of these defects were observed in the present study also (Figs.2-5). Origin of these defects is not completely understood. In the Zr based alloy such alignment of defects has been noticed when fluence of high energy (>0.1MeV) exceeds 10^{26} neutron/m^2 [11,17,20].

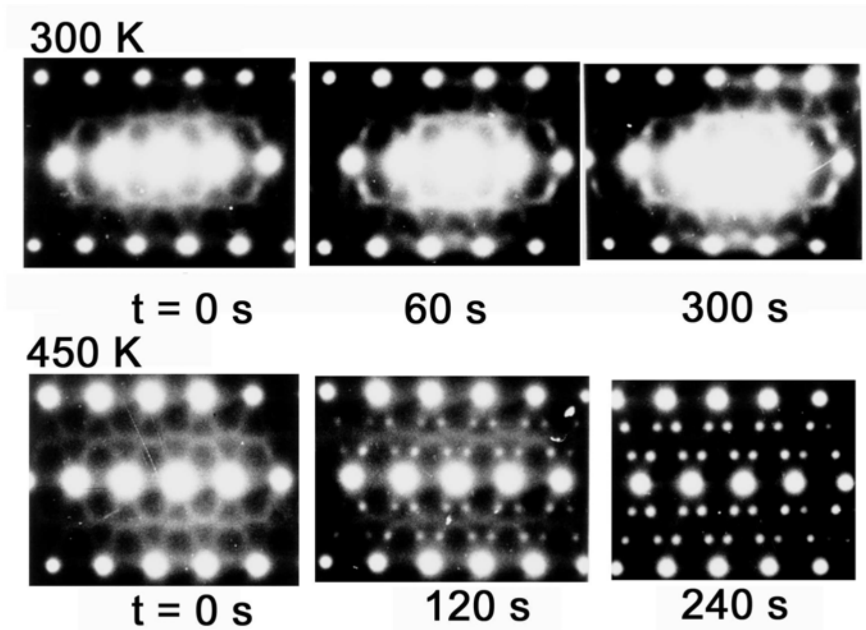

Fig. 6. *Selected area diffraction patterns from the β-phase regions after irradiating with 1 MeV electrons for different time periods. Gradual transformation of the diffuse intensity to the ω reflections could be noticed.*

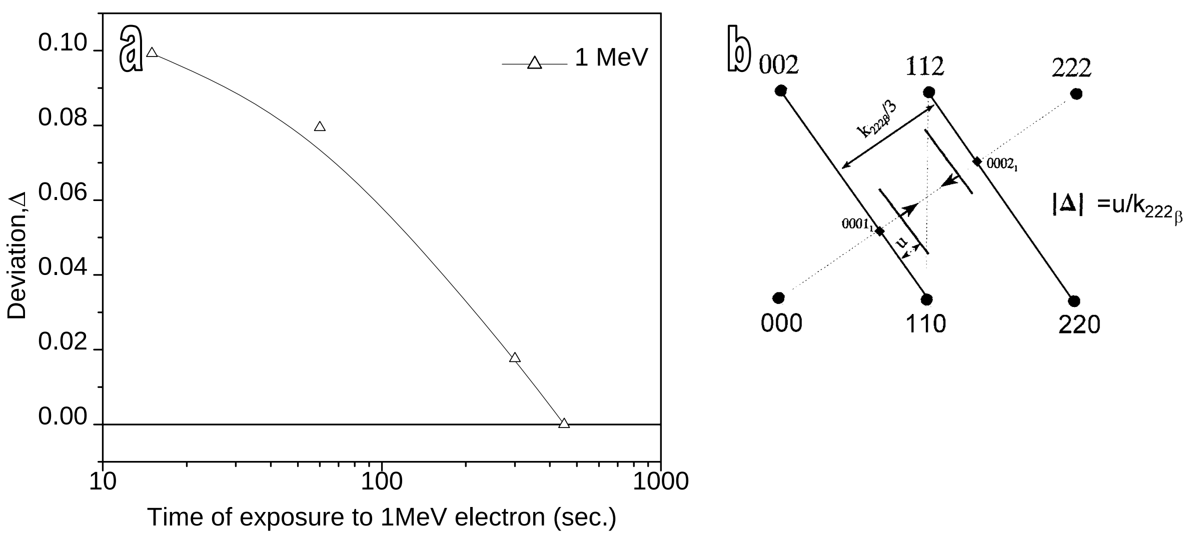

Fig. 7 (a) showing quantitative estimate of the rate of formation of the ω phase with exposure to electron irradiation.(b) The schematic presentation showing methodology to estimate the deviation parameter.

All these observations suggest that these defects align in low strain energy configuration. It has been suggested that the origin of these bands is due to the accumulation of the interstitials on (0002) planes. With increase in the concentration these interstitials form loop on (0002) planes.

Upon further increase in concentration, alignment of defects on other crystallographic orientations may start in order to minimize the over all strain energy. Some times these alignments also exhibit '*corduroy contrast*' which arises due to the misorientation of the small crystal regions causing the periodical variation in the Bragg position which give rise to the ordered dark and light contrast due to which band like morphology appears in the microstructure. When oxygen ions having energy of 116 MeV were bombarded on the target comprising of zirconium based alloys, typical range of penetration of these ions is nearly 66 μm. Hence most of the deformation is confined within this region. Beyond this range oxygen ions will get entrapped into the material and should remain in solution. Upon examination of the sample by 'focused ion beam' from a region in the direction of the path traverse by ion beam, track of ions could be noticed under high angle annular dark field, where due to large defects accommodate in the path of track show a contrast different from the matrix phase (Fig.3). In Zr-1 Nb sample, where the β precipitate is not in equilibrium condition, irradiation induce defected provide earlier attainment of the growth of the β phase. It , therefore can be inferred that the morphology of the β phase will undergo substantial changes under irradiation.
The energy imparted by the high energy electrons, on the other hand, give rise to a large number of smaller omega embryos, in comparison to comparatively global uniform temperature induced omega formation (also known as thermal omega). The thermal induced transformation appears to progress in more orderly fashion in comparison to the irradiation induced transformation which being inherently a localized phenomenon resulting in localized defects. Thus, the possibility of formation of higher structural variants (ω_5,ω_7) is more probable in case of irradiation leading to larger peak shift or $|\Delta|$. Another striking feature noted from the streak length plot was the larger spread of values about mean in case of irradiation induced ω than the thermal ω. This further indicates that, the internal order of ω structural units inside the irradiation induced ω is lower in extent in comparison to thermal ω. This could again be an outcome of the random nature of irradiation, which results in lower internal order among various ω structural units. A detailed analysis of this finding is planned to be published in another paper.

5. Conclusions

Effect of irradiation by ions has been studied in various zirconium based alloys. Different defects and phase formed by irradiation have been identified. Bombardment with ions manifests in a variety of defects in the microstructures. In case of zircaloy-2 samples majority of the defects were in form of the deformation bands. Formation of these deformation bands is attributed to the condensation of defects on certain crystallographic planes. Upon electron irradiation, the β phase showed tendency for the formation of the ω phase. Though the orientation relationship of the phase with the β phase was same as that of observed in the case of thermal treatment, there was subtle differences observed in the distribution of diffuse intensity observed in SAD patterns. Simulations carried out showed that such difference could be due to possible arrangements of subunits in both the phases.

References

1. H. Ullmaier, W. Schilling, IAEA-SMR-46/105.
2. M. Griffiths, J. Nucl. Mat., 159(1988)190.
3. H. Ullmaier, Trans-IIM, 34(1981)324.
4. R. W. Gilbert, K. Farrell and C. E. Coleman, J. Nucl. Mat., 84(1979)137.
5. B. N. Singh, S. I. Golubov, H. Trinkaus, D. J. Edwards and M. Eldrup, J. Nucl. Mat., 328(2004)77.
6. L. M. Howe, D. Phillips, A. T. Motta and P. R. Okamoto, Surface and Coatings Tech., 66(1994) 411.
7. L. Pagano Jr., A. T. Motta and R. C. Birtcher, J. Nucl. Mat. 244 (1997) 295.
8. C. Abromeit, H. Wollenberger, S. Matsumura and C. Kinoshita, Nucl. Mat., 276(2000)104.
9. L. M. Howe, M. H. Rainville, D. Phillips, H. Plattner and J. D. Bonnett, N. Ins. Meth. Phys. Res. B80/81 (1993)73.
10. T. D. Gulden and I. M. Bernstein, Phil. Mag., 14 (1968) 1087.
11. D. Lee, E. F. Koch and J. H. Rosolpwski, J. Nucl. Mater. 50 (1974) 162.
12. R. S. Nelson, D. J. Mazey and J. A. Hudson, J. Nucl. Mater., 37(1970)1.
13. D. Pecheur, F. Lefebvre, A. T. Motta and C. Lemaignan, J. Nucl. Mater. 189(1992).318.
14. L. Pagano Jr., A. T. Motta, R. C. Birtcher, J. Nucl. Mater. 244 (1997) 295.
15. C. D. Williams and R. W. Gilbert, Radiat. Eff., 22 (1974)139.
16. P. Mukherjee, P. Barat, S. K. Bandopadhyay, P. Sen, S. K. Chattopadhyay, S. K. Chatterjee, M. K. Mitra, J. Nucl. Mater. 305 (2002) 169.
17. T. Y. Yang, G. P. Yu and L. J. Chen, J. Nucl. Mater. 150 (1987) 67.
18. The stopping and Range of Ions in Matter (SRIM 2000) software developed by J. Ziegler and J. P. Biersack is available on website http://www.research.ibm.com/ionbeam.
19. X. W. Chen, X. D. Bai, P. Y. deng, Q. G. Zhou, R. H. Yu and B. S. Chen, Vacuum , 72(2004)467.
20. F. Onimus, I. Monnet, J. L. Bechade, C. Prioul and P. Pilvin, J. Nucl. Mater. 328 (2004) 165.
21. M. Griffiths, R. A. Holt and R. Rogerson, J. Nucl. Mater. 225 (1995) 245.
22. O. T. Woo and G. J. C. Carpenter, J. Nucl. Mater., 159 (1988) 397.
23. W. L. Bell, J. Nucl. Mater. 55 (1975) 14.
24. A. V. Nikilina, V. A. Markelov, M. M. Peregud, V. N. Voevodin, V. L. Panchenko, G. P. Kobylyansky, J. Nucl. Mater., 238(1996)205.